

# Supraglacial lakes on the Larsen B ice shelf, Antarctica, and at Paakitsoq, West Greenland: a comparative study

Alison F. BANWELL,<sup>1,2</sup> Martamaria CABALLERO,<sup>3,1</sup> Neil S. ARNOLD,<sup>2</sup>  
Neil F. GLASSER,<sup>4</sup> L. Mac CATHLES,<sup>1</sup> Douglas R. MacAYEAL<sup>1</sup>

<sup>1</sup>*Department of Geophysical Sciences, University of Chicago, Chicago, IL, USA*

*E-mail: afb39@cam.ac.uk*

<sup>2</sup>*Scott Polar Research Institute, University of Cambridge, Cambridge, UK*

<sup>3</sup>*Centro Mario Molina Chile, Santiago, Chile*

<sup>4</sup>*Centre for Glaciology, Institute of Geography and Earth Sciences, Aberystwyth University, Aberystwyth, UK*

**ABSTRACT.** Supraglacial meltwater lakes trigger ice-shelf break-up and modulate seasonal ice-sheet flow, and are thus agents by which warming is transmitted to the Antarctic and Greenland ice sheets. To characterize supraglacial lake variability we perform a comparative analysis of lake geometry and depth in two distinct regions, one on the pre-collapse (2002) Larsen B ice shelf, Antarctica, and the other in the ablation zone of Paakitsoq, a land-terminating region of the Greenland ice sheet. Compared to Paakitsoq, lakes on the Larsen B ice shelf cover a greater proportion of surface area (5.3% cf. 1%), but are shallower and more uniform in area. Other aspects of lake geometry (e.g. eccentricity, degree of convexity (solidity) and orientation) are relatively similar between the two regions. We attribute the notable difference in lake density and depth between ice-shelf and grounded ice to the fact that ice shelves have flatter surfaces and less distinct drainage basins. Ice shelves also possess more stimuli to small-scale, localized surface elevation variability, due to the various structural features that yield small variations in thickness and which float at different levels by Archimedes' principle.

**KEYWORDS:** Antarctic glaciology, Arctic glaciology, ice-shelf break-up, ice shelves, surface melt

## 1. INTRODUCTION

Supraglacial lake dynamics have become an increasingly important factor in ice-sheet response to climate change, because lakes have been implicated in ice-shelf disintegration (e.g. Scambos and others, 2003) and influenced grounded ice-sheet flow through their impact on subglacial hydrology. When lakes on ice sheets suddenly drain (e.g. Das and others, 2008; Doyle and others, 2013; Tedesco and others, 2013), the subglacial drainage system receives a pulse of water that, in turn, contributes to both temporary and longer-term changes in ice velocity (Bartholomew and others, 2011; Hoffman and others, 2011; Banwell and others, 2013; Joughin and others, 2013). Within the ablation zone of the Greenland ice sheet (GrIS), supraglacial lakes form in surface depressions controlled by the interplay between bedrock topography and ice flow (Echelmeyer and others, 1991; Darnell and others, 2013; Sergienko, 2013). This means that processes unrelated to climate change (i.e. bedrock characteristics and ice-flow physics) determine the areal distribution, maximum depth and volume of the lakes.

In contrast, lakes on floating ice shelves do not depend on the ice/bedrock interaction to define their location, geometry and volume. Instead, lakes on ice shelves inhabit various surface depressions that arise from a variety of processes (e.g. basal crevassing (McGrath and others, 2012), grounding zone flow-stripe development (Glasser and Gudmundsson, 2012) and intermittent suture-zone voids (Glasser and others, 2009)). Lakes on ice shelves are also products of the viscoelastic flexure of the ice, and can represent a surface load that can suddenly change when fractures develop through the ice shelf, causing lake drainage through hydrofracture (Van der Veen, 1998, 2007; MacAyeal and Sergienko, 2013).

Among the impacts of supraglacial lakes on both grounded and floating ice, none are so powerfully linked to ice-sheet change as those leading to the sudden collapse of the Larsen B ice shelf (LBIS), Antarctica, in 2002 (e.g. Scambos and others, 2000, 2003; Van den Broeke, 2005; Vaughan, 2008). During the decades leading up to the collapse, the number of lakes on the central portion of the ice shelf gradually grew from near zero to ~3000 (Scambos and others, 2000; Glasser and Scambos, 2008). However, just days prior to the disintegration, the majority of the ~3000 lakes drained, suggesting that the sudden, coordinated movement of surface water to the ocean below may have been a contributing proximal trigger to the collapse (Scambos and others, 2003). The loss of the majority of the LBIS resulted in a reduction of the buttressing forces that act to reduce ice flow across grounding lines shared with the ice shelf. Following the break-up event, a sustained speed-up of land-to-sea ice flow of glaciers that were previously buttressed by the ice shelf was observed (Scambos and others, 2000, 2004; Sergienko and MacAyeal, 2005; Van den Broeke, 2005; Glasser and Scambos, 2008; Glasser and others, 2011; Rott and others, 2011). Thus, as with the acceleration of GrIS flow, the inland ice of Antarctica can also accelerate in response to lake drainage, but by a different mechanism.

However, while ground-based studies of supraglacial lakes on the GrIS are abundant, relatively little ground-based research has been directed toward study of supraglacial lakes on Antarctic ice shelves. Antarctic lakes are harder to study because they are either more remote (relative to logistics centres) or have themselves disappeared as the ice shelves on which they resided no longer exist.

In the present study, we endeavour to strengthen the link between the relatively plentiful research directed to lakes on

the GrIS and the relatively unstudied lakes on the present and recently collapsed ice shelves of Antarctica. The first step in establishing this link is to determine parallels and contrasts between spatial patterns, shapes, surface areas and depths of lakes on the land-terminating Paakitsoq region of the GrIS and on the former LBIS. Our study is conducted through the analysis of Landsat 7 Enhanced Thematic Mapper Plus (ETM+) imagery acquired for both regions.

In addition to improving our overall understanding of supraglacial lakes on ice shelves, this study will help to establish whether or not surface-routing and lake-filling models which are already in existence for the GrIS (e.g. Banwell and others, 2012a; Leeson and others, 2012) are transferable to Antarctic ice shelves. Finally, our work will establish idealized properties of supraglacial lake geometries; an important first step in the development of numerical model studies of lakes on ice sheets and ice shelves.

## 2. METHODS

In this section we describe the analytical process that was undertaken for both the LBIS, and for a similar-sized (~3000 km<sup>2</sup>) area of grounded ice in the Paakitsoq region of the GrIS, northeast of Jakobshavn Isbræ (Banwell and others, 2012b, their fig. 1). Two Landsat 7 ETM+ images were analysed for this study. For the LBIS, we chose the image dated 21 February 2000 (scene ID: L71216106\_10620000221), as this is the most cloud-free image available within 2 years of the break-up event. This image also forms the basis of a prior study of lake patterning and morphology on the LBIS (Glasser and Scambos, 2008), and thus serves as a fiduciary representation of the state of the LBIS 2 years prior to its collapse. For Paakitsoq, Greenland, we used the cloud-free image dated 7 July 2001 (scene ID: L71009011\_01120010707). We note that the two images are from periods of time during the melt season that do not coincide with either 'time of maximum lake volume' or 'end of season' or any other benchmark, but are rather snapshots of time that represent the best available information.

### 2.1. Lake boundaries and area

Image pixels were classified into 'lake-covered' or 'bare ice/snow' using Landsat image reflectance data, following Box and Ski (2007). Each Landsat band was first converted from digital numbers to radiance and then from radiance to reflectance using the equations of Chander and others (2009). Then, to make this classification, the blue/red ratio of reflectance (involving Landsat bands 1 and 3; 450–515 and 630–690 nm, respectively) was evaluated from the Landsat image. As this ratio increases toward the lake centres, where water is deepest, and decreases towards the edges, where water is most shallow, it was necessary to carefully identify the value of this ratio corresponding to bare ice at lake edges. Based on experimental results, and on known areas of lakes on the GrIS, Box and Ski (2007) suggest that the threshold value of blue/red ratio of reflectance should be in the range 1.05–1.25 at the edges of lakes. Further to the study by Box and Ski (2007), we found that the algorithm needs to be adapted to avoid problems associated with floating lake ice on lake surfaces. Unless these areas were masked, negative lake depths were found, due to the high reflectance of the ice compared to the open water.

Once the pixels representing flooded areas had been established, the 'bwboundaries' function in MATLAB was

used to identify lake boundaries. Subsequently, the 'regionprops' function in MATLAB was used to identify the number of pixels (i.e. surface areas of lakes) within the closed edges as a means of determining lake area.

### 2.2. Lake depth

Supraglacial lake depths were estimated using a method developed by Sneed and Hamilton (2007), originally applied to Advanced Spaceborne Thermal Emission and Reflection Radiometer (ASTER) (VNIR1, 520–600 nm) imagery, but also applicable to Landsat 7 ETM+ imagery (band 2; 525–605 nm) (Sneed and Hamilton, 2011). The approach for extracting water depth and lake-bottom albedo is based on the Beer–Lambert law (Ingle and Crouch, 1988), which describes the attenuation of radiation through a water column:

$$I(z, \lambda) = I(0, \lambda)e^{-(K_\lambda)(z)}, \quad (1)$$

where  $I(z, \lambda)$  is the water-leaving spectral intensity at some depth,  $I(0, \lambda)$  is the spectral intensity at zero depth,  $K_\lambda$  is the spectral attenuation and  $z$  is depth. Written in terms of reflectance, and inverted to logarithmic form (Philpot, 1989),  $z$  is determined by

$$z = \frac{[\ln(A_d - R_\infty) - \ln(R_w - R_\infty)]}{1 - g}, \quad (2)$$

where  $A_d$  is the bottom or substrate albedo (reflectance),  $R_\infty$  is the reflectance for optically deep water,  $R_w$  is the reflectance of some pixel of interest and  $g$  is given by

$$g \approx K_d + aD_u, \quad (3)$$

where  $K_d$  is the diffuse attenuation coefficient for downwelling light,  $a$  is the beam absorption coefficient and  $D_u$  is an upwelling light distribution function or the reciprocal of the upwelling average cosine (Mobley, 1994).

To determine  $A_d$  we took the mean reflectance value of the ring of pixels around the lake that are barely covered with water (i.e. those adjacent to the water-covered pixels, as detected by the blue/red ratio of reflectance). Although Sneed and Hamilton (2007) used the same  $A_d$  for their entire region of interest, as our region is larger we chose to calculate a unique  $A_d$  for each lake. For the LBIS, values for  $A_d$  ranged from 0.30 to 0.79 (with a mean value of 0.68), and for Paakitsoq, values for  $A_d$  ranged from 0.17 to 0.76 (with a mean value of 0.66).

To determine  $R_\infty$ , the reflectance from optically deep water where the influence of bottom reflectance is nil, we used the value of reflectance from water that is deeper than ~40 m in the image. It was necessary to take care when selecting pixels that were far from shorelines, to ensure that  $R_\infty$  estimates were not biased by water that was too shallow, turbid water or pixels containing floating ice.

This approach assumes that the substrate (bottom) of the lake is homogeneous, the impact of suspended or dissolved organic or inorganic matter in the water column is negligible on absorption, there is no inelastic scattering (e.g. Raman scattering or fluorescence) and that the lake surface is not significantly roughened due to wind (Sneed and Hamilton, 2007). Once the depth of each 'flooded' pixel had been calculated, the 'regionprops' function in MATLAB was again used to determine the 'MaxIntensity' (i.e. the maximum lake depth) and the 'MeanIntensity' (i.e. the mean lake depth) for each of the identified lakes.

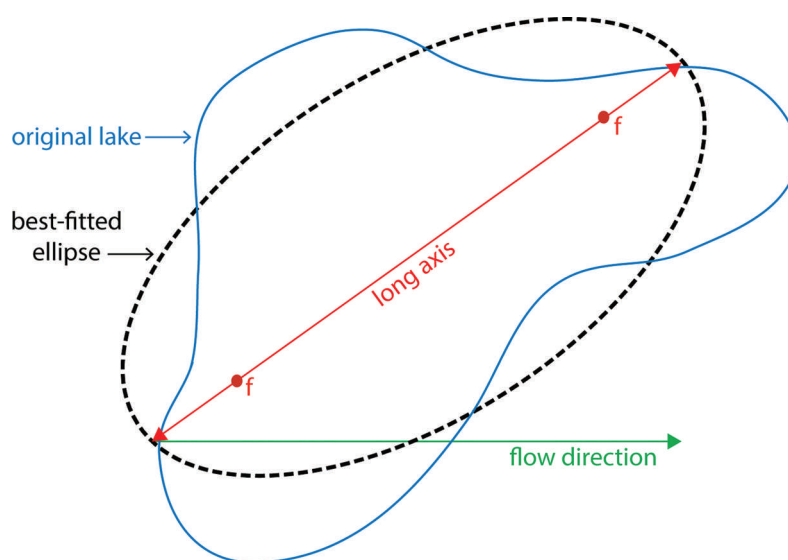


**Fig. 1.** Schematic of optimal fit of an ellipse (with  $f$  indicating the foci) to the outline of a previously identified lake. The ellipse and original lake are equal in area. The angle between the long axis of the ellipse and the flow direction (either clockwise or anticlockwise) determines the ellipse orientation.

### 2.3. Lake shape, orientation and eccentricity

Once lake edges, and thus areas, had been delineated (following Box and Ski, 2007), and depths had been established (following Sneed and Hamilton, 2007), the MATLAB 'regionprops' function was used to obtain other lake properties. As illustrated in Figure 1, this function works by best-fitting ellipses to the identified lakes. Lake properties which this function is able to diagnose include: (1) eccentricity (i.e. the ratio from 0 to 1 of the distance between the foci of the ellipse and its long axis length, where 0 indicates that the ellipse is a circle and 1 indicates a line segment), (2) orientation (from  $0^\circ$  to  $90^\circ$  from the average ice-flow direction on the ice shelf/sheet in either a clockwise or anticlockwise direction) and (3) solidity (from 0 to 1, denoting the proportion of the pixels in the convex hull of the lake that are also bound within the lake itself; lakes with sinuous boundaries tend to have low solidity, circular lakes have a solidity of 1).

### 2.4. Algorithm validation

Using the same 21 February 2000 image, Glasser and Scambos (2008) produced a detailed structural glaciological analysis of overall changes in surface structures on the LBIS prior to its collapse in late February 2002. Although this study, which used manual digitization, identified general patterns of lake positions, areas and shapes of supraglacial lakes, it did not perform a quantitative analysis of these properties and, importantly, did not analyse lake depth. Thus, in our study, we also statistically analyse the shape files of lakes used in the Glasser and Scambos (2008) study, in order to compare, and thus validate, the results of our study using an automated algorithm.

## 3. RESULTS

### 3.1. Larsen B lake patterns and characteristics

The most appropriate value for the blue/red band threshold for the LBIS to appropriately discriminate bare ice/snow from water is found to be 1.2, which results in the identification of 3227 lakes, as shown in Figure 2. This

threshold value is chosen because it produces a pattern of lakes on the ice-shelf surface that is most similar to the pattern of lakes identified visually on the Landsat image and documented by Glasser and Scambos (2008) (also see Section 3.2). If a slightly lower threshold value of 1.1 is chosen, only 272 separate flooded areas are identified, as the majority of the entire surface of the LBIS is erroneously classified as lake-covered. If a slightly higher threshold value of 1.3 is chosen, only 1419 lakes are identified, and the small lakes, in particular, are no longer identified.

As also recognized by Glasser and Scambos (2008), we identify a variety of different 'domains' on the ice-shelf surface, each displaying different lake characteristics. We have highlighted lakes within three areas of these domains in Figure 2. In area a of Figure 2, we see fairly linearly shaped lakes, with their long axis diverging from the mean ice-flow direction from west to east. This is indicative of ice-flow divergence where fast-flowing glaciers enter the ice shelf from the west. Although lake depths generally vary from  $\sim 1$  to  $\sim 4$  m here, the deepest identified lake on the ice shelf also falls within this region; calculated to be 6.8 m at its deepest point. In area b of Figure 2, longitudinal features, which are aligned roughly parallel with ice flow, dominate. These features are up to 30 km in length and 2–3 m in depth. Thus, compared to area a, ice flow in this region is likely to be convergent rather than divergent along the flow direction. In area c of Figure 2, we see lakes that are fairly circular (i.e. their eccentricity is close to 1) and have a larger mean area than the majority of lakes on the ice shelf. We suggest that these characteristics are due to slower ice flow in this region (for additional information on structural features of the LBIS related to flow, as well as the area of the LBIS that disintegrated, refer to Glasser and Scambos, 2008). Through an increased lifespan, lakes would be able to undergo more enlargement by bottom ablation than other lakes on the ice shelf. The majority of the lakes in this area are also covered with floating ice (seen as white areas in Fig. 2c). Although the outer rings of open, lake-ice-free water of the lakes are calculated to be from  $\sim 0.5$  to  $\sim 1.5$  m in depth, we cannot calculate the depth of the central, probably deepest, regions because of the ice cover.

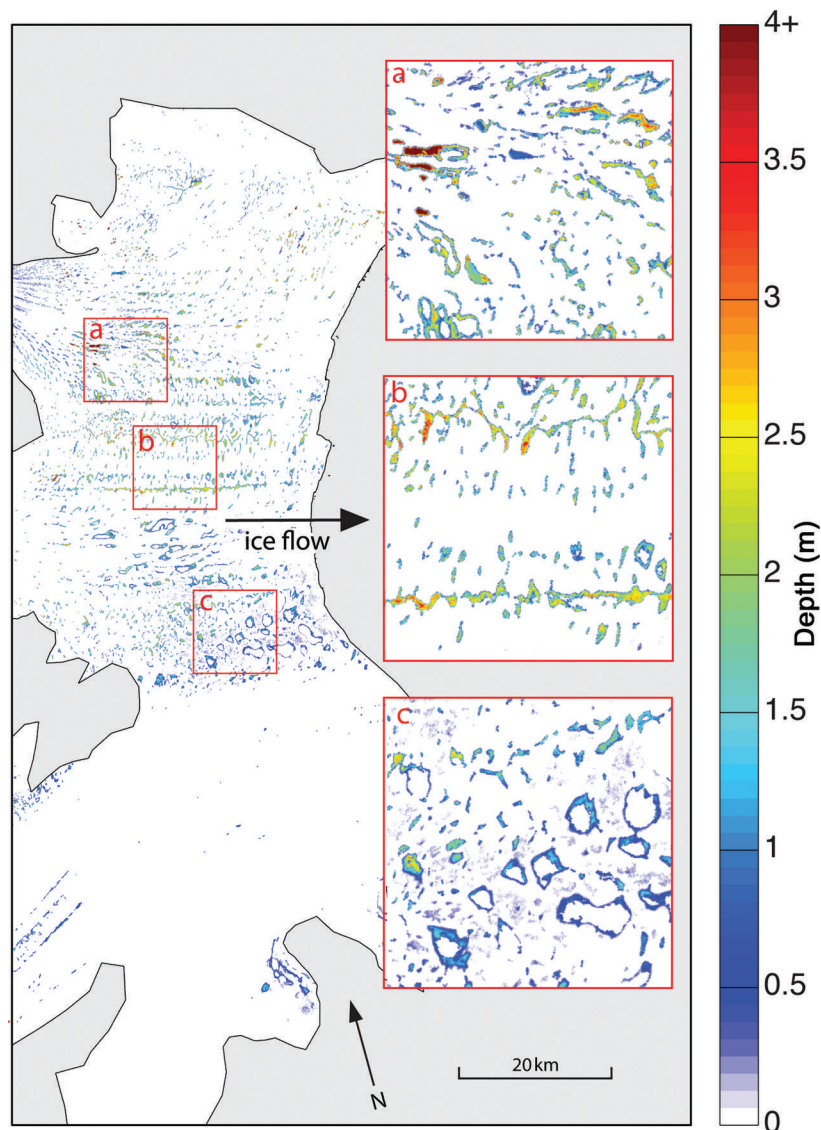


**Fig. 2.** Depths of lakes on the Larsen B ice shelf using reflectance of the 21 February 2000 Landsat image. Although some lake depths are  $>4$  m, for visualization purposes 4 m is plotted as the maximum depth here. Three areas, a, b and c, are enlarged to show varying lake characteristics and patterns across the ice-shelf surface. Marginal areas, which can be grounded ice, bare land surface or ocean surface, are shaded grey.

Over the entire ice shelf, we calculate the mean lake area to be  $0.10 \text{ km}^2$  (with standard deviation,  $\sigma = 0.29 \text{ km}^2$ ) and the total surface area covered by lakes to be  $315 \text{ km}^2$ . This is 5.3% of the total area of ice shelf analysed, with a mean lake density of  $0.55 \text{ km}^{-2}$ . We calculate that lakes covered  $\sim 10\%$  of the  $3200 \text{ km}^2$  of ice shelf which disintegrated in a 35 day period beginning on 31 January 2002 (Scambos and others, 2004). As we discuss below, this larger percentage of lake cover constitutes one of the most important differences between lakes on the LBIS and lakes on the GrIS.

The mean lake depth on the LBIS is calculated to be  $0.82 \text{ m}$  ( $\sigma = 0.56 \text{ m}$ ), and the mean maximum lake depth is  $1.6 \text{ m}$  ( $\sigma = 0.99 \text{ m}$ ) (Fig. 3). The mean eccentricity is  $0.84$  ( $\sigma = 0.13 \text{ m}$ ), the mean solidity is  $0.80$  ( $\sigma = 0.14$ ) and the average mean orientation of the long axis of ellipses (best-fitted to the lakes) is  $46^\circ$  away from the flow direction ( $\sigma = 28^\circ$ ). The latter assumes that the average flow direction is from west to east (Vieli and others, 2006, their fig. 5).

Using the mean lake depth ( $0.82 \text{ m}$ ), the total number of lakes on the LBIS (3227), the average lake area ( $0.1 \text{ km}^2$ ) and the assumption that the ice shelf has a uniform thickness

of  $200 \text{ m}$  (Sandhäger and others, 2005), we calculate that there are  $5.2 \times 10^8 \text{ MJ}$  of potential energy stored on the surface as free water (equivalent to  $8.7 \times 10^4 \text{ MJ km}^{-2}$ ). This calculation is useful, as it gives an indication of the amount of energy available for the drainage of lakes by hydrofracture, the process that was probably the main driver behind the disintegration of the ice shelf (Scambos and others, 2003, 2009).

### 3.2. Comparison to results of the Glasser and Scambos (2008) study

Glasser and Scambos (2008) identified 2696 supraglacial lakes (their 'meltwater ponds'); 16% fewer than the number of lakes identified in our study. Glasser and Scambos (2008) also calculated that individual lakes had a slightly higher mean area of  $0.13 \text{ km}^2$ , and in total they calculated that lakes on the LBIS covered a slightly higher surface area of  $365 \text{ km}^2$ . However, although we calculate that lakes are on average  $\sim 30\%$  smaller than the lakes identified by Glasser and Scambos (2008), as we identify  $\sim 16\%$  more lakes on the LBIS we calculate that the total surface area of lake

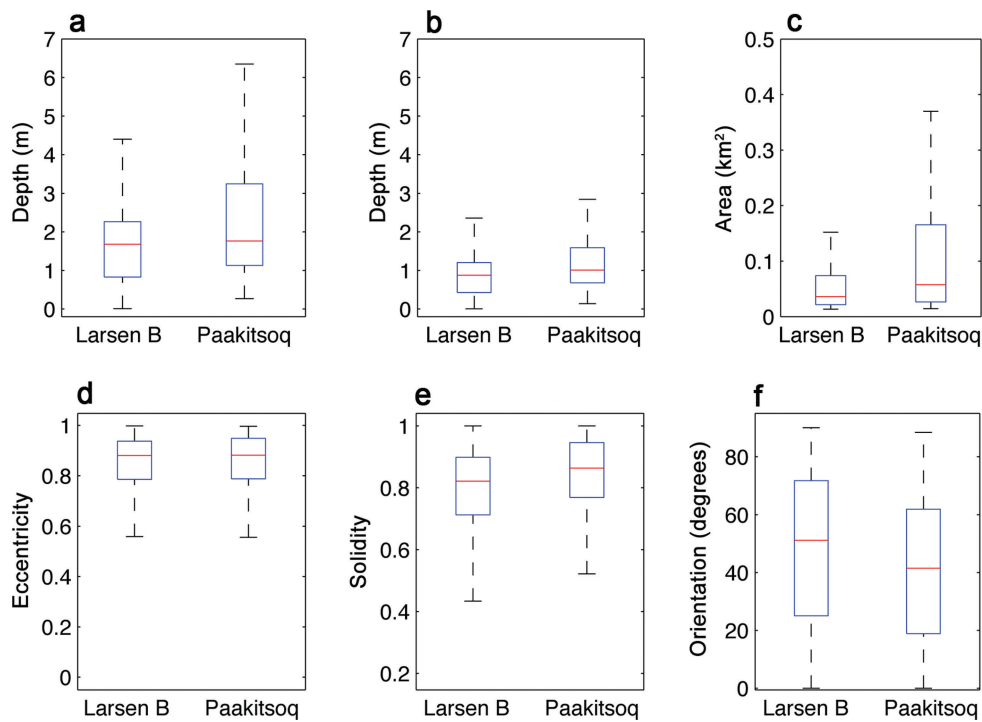


**Fig. 3.** Plots showing (a) maximum depth, (b) mean depth, (c) mean area, (d) eccentricity, (e) solidity and (f) orientation from the mean flow direction, of lakes on both the LBIS ( $N = 3227$ ) and at Paakitsoq ( $N = 239$ ) in order to clearly capture the scale and differences between the two lake systems. On each box the red mark is the median and the edges of the box are the 25th and 75th percentiles ( $q_1$  and  $q_3$ , respectively). The length of the whiskers (dotted lines) is equal to  $q_3 + 1.5(q_3 - q_1)$ .

coverage is only  $\sim 12\%$  less than that calculated by Glasser and Scambos (2008).

### 3.3. Comparison with a land-terminating region of the GrIS

Compared to the threshold value for the blue/red ratio for the LBIS, a slightly higher threshold value of 1.4 is required for the Paakitsoq region of the GrIS. Using this threshold value, we identified 239 lakes, as shown in Figure 4 (note a different depth scale than Fig. 1). Threshold values  $< 1.4$  for Paakitsoq result in large, dispersed areas of the ablation zone being erroneously classified as lakes. Threshold values  $> 1.4$  for Paakitsoq meant that the wispy, linear water features, observed to link lakes in the areas of higher elevation within the region studied (Fig. 4, area b), were no longer identified as flooded areas.

Figure 3 compares the values of key lake properties between the LBIS and the Paakitsoq region. Compared to lakes on the LBIS, lakes in the Paakitsoq region have a larger mean area of  $0.15 \text{ km}^2$  ( $\sigma = 0.24 \text{ km}^2$ ). However, we calculate that lakes only cover  $\sim 1\%$  of the ice surface compared to  $5.3\%$  for the LBIS. The mean lake density in the Paakitsoq region is thus only  $0.07 \text{ km}^{-2}$ . This constitutes one of the major differences between lakes on grounded ice and floating ice we have identified in the comparison.

Lakes in the Paakitsoq region are also generally deeper than lakes on the LBIS, with a mean depth of  $1.3 \text{ m}$  ( $\sigma = 0.97 \text{ m}$ ) and a mean maximum depth of  $2.5 \text{ m}$  ( $\sigma = 1.9 \text{ m}$ ) (Figs 3 and 4). The deepest identified lake in the region, calculated to have a maximum depth of  $9.0 \text{ m}$ , is shown in area a of Figure 4. Overall, lake depths across the Paakitsoq region show more variation than the lakes on the LBIS (Fig. 3). With regard to the lake orientations, LBIS lakes are on average orientated  $46^\circ$  away from the dominant ice-flow

direction, whereas the average orientation of Paakitsoq lakes from the dominant flow direction (east to west) is  $37^\circ$  ( $\sigma = 24^\circ$ ). The calculated solidity for the Paakitsoq lakes is  $0.83$  ( $\sigma = 0.15$ ), which is  $4\%$  higher than the value for the LBIS lakes (i.e. Paakitsoq lakes are more convex than LBIS lakes).

## 4. DISCUSSION

When average values for lake properties identified in our study are compared to those of lakes identified by Glasser and Scambos (2008), it is encouraging that the total number of lakes and the average area of those lakes are of the same order of magnitude for both studies. There are, however, some minor discrepancies. For example, we identify  $16\%$  more lakes than Glasser and Scambos (2008), and those lakes are on average  $30\%$  smaller. Thus, it is likely that the analysis of Glasser and Scambos (2008) may have grouped together into one large lake what our automated algorithm identified as a collection of nearby smaller lakes.

The automated algorithm used in our study extends the Glasser and Scambos (2008) study by also calculating lake depths. Glasser and Scambos (2008) state that, although supraglacial lakes are generally aligned along the local topographic slope (which is roughly aligned perpendicular to the general ice-flow direction), some surface water features are longitudinal in form and are aligned parallel to the downslope direction. Although they suggest that these features could be interpreted as meltwater streams, as have been observed on the Amery Ice Shelf, Antarctica (Phillips, 1998), such a deduction does not agree with all other observations. For example, as we calculate these features to be  $\sim 2 \text{ m}$  or more deep (Fig. 2, area b, displayed in light green), we suggest that they are unlikely to all be meltwater streams, as many do not reach the eastern edge of the ice

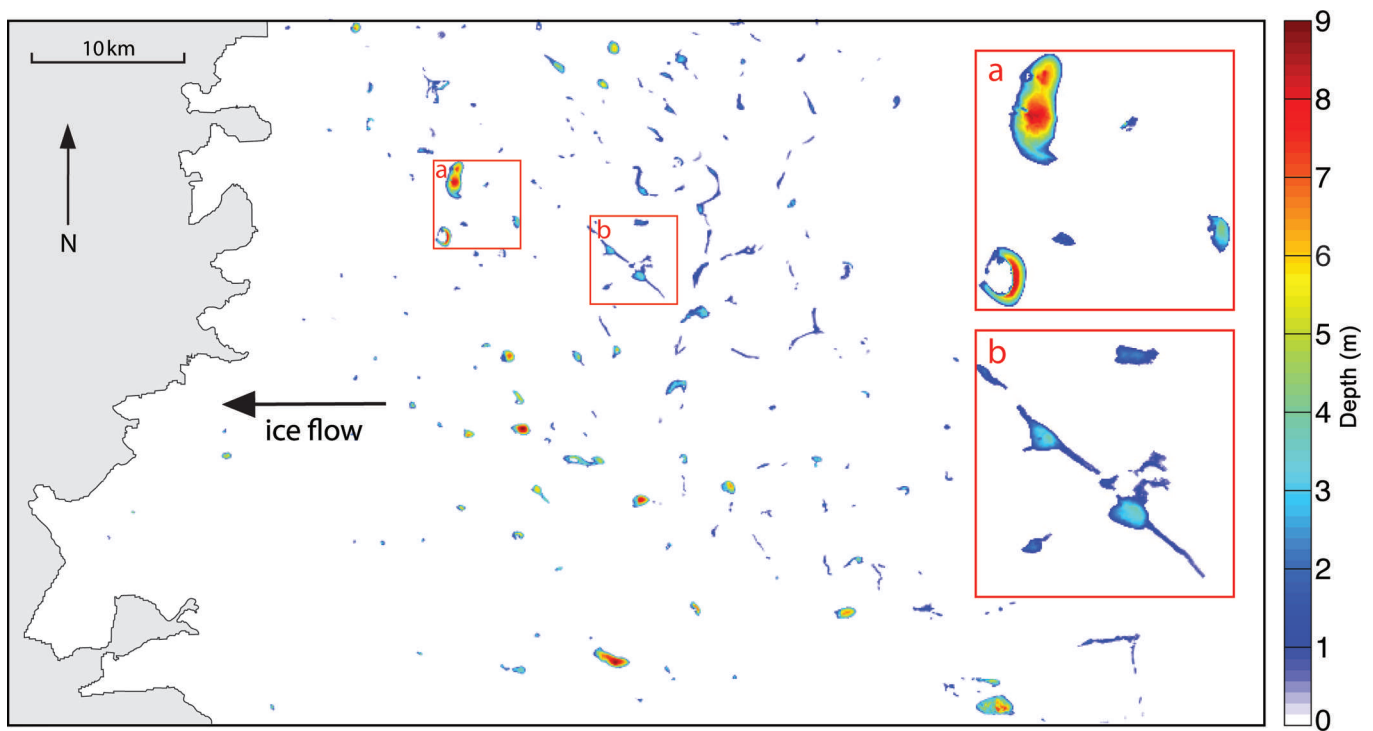


**Fig. 4.** Depths of lakes in the Paakitsoq region, West Greenland (see Banwell and others, 2012b, for location figure) using reflectance of the 7 July 2001 Landsat image. Two areas, a and b, are highlighted, in order to show varying lake characteristics and patterns across the ice-sheet surface. Marginal areas of bare land surface are shaded grey.

shelf and thus there is not an obvious outflow point for a large quantity of water to leave the ice shelf (unless outflow is accommodated by a moulin). Additionally, as the ice-shelf surface slope is minimal (i.e. the ice thickness change from grounding line to ice front is  $\sim 50$  m (Sandhäger and others, 2005, their fig. 2), implying a 5 m change in  $\sim 50$  km, or a slope of  $10^{-4}$ ), it seems unlikely that there could be a substantial volume of flowing water across the ice-shelf surface. Thus, although some meltwater has been observed to leave the LBIS as waterfalls (personal communication from T. Scambos, 2013), this runoff into the ocean is likely to be only a small fraction of the summer surface melt volume.

The standard deviations and interquartile ranges of mean lake depth, maximum lake depth and lake area are generally higher in the Paakitsoq region, indicating that Paakitsoq lakes have more variable depths and areas than LBIS lakes (Fig. 3). The reason for this is likely to be primarily related to the substantial elevation gradient in the Paakitsoq region: from  $\sim 400$  m at the ice margin to 1500 m inland, compared to an almost negligible elevation gradient on the floating LBIS. Consequentially, on the GrIS, increased melt as summer progresses not only causes existing lakes to grow, but also results in lake formation at higher elevations as the ablation zone expands (Liang and others, 2012; Fitzpatrick and others, 2013). Conversely, the standard deviations of eccentricity, orientation and solidity are found to be comparable between the two regions. This is because these lake properties are affected by elevation to a much lesser extent than lake depth and area.

The mean depth of Paakitsoq lakes is calculated to be 0.48 m more than for lakes on the LBIS, and the mean maximum depth of Paakitsoq lakes is calculated to be 0.90 m more than LBIS lakes (Fig. 3). Additionally, Paakitsoq lakes are on average  $0.05$  km<sup>2</sup> larger than LBIS lakes. A less striking difference between lakes in the two regions

concerns their average orientation. We calculate that Paakitsoq lakes are orientated at a lower angle ( $37^\circ$ ) to the average ice flow direction than the LBIS lakes ( $46^\circ$ ). These differences are thought to be due to a variety of different reasons, discussed below.

We suggest that the differences in average lake depth and area are partially due to the higher surface melt rates on the GrIS. Owing to its size and elevation, the Antarctic ice sheet creates its own climate with an important influence on the surrounding ocean (Rignot and Thomas, 2002; Bromwich and others, 2013). Furthermore, once a lake exists, it enlarges not only by receiving meltwater from the surrounding ice surface, but also due to a positive albedo feedback process, whereby bottom-lake ablation is enhanced by up to 170% compared to bare ice, as modelled by Lüthje and others (2006), and up to 135%, as observed by Tedesco and others (2012).

The other reason for the differences in average lake depth, area and orientation between the two locations relates to the two fundamentally different ways in which supraglacial lakes on land-terminating regions of the GrIS and on Antarctic ice shelves initially form and subsequently interact with one another. At Paakitsoq, supraglacial lakes form in surface depressions that are controlled by the underlying bedrock topography (Box and Ski, 2007; Lampkin and Vanderberg, 2011) and by spatial variations in the degree of basal ice lubrication and sliding velocity (Gudmundsson, 2003). This causes the majority of lakes on the GrIS to remain in fixed locations interannually (Thomsen and others, 1988; Echelmeyer and others, 1991; Selmes and others, 2011), and thus the average orientation and volume of lakes in a specific region of the GrIS will depend on the average patterns of bed topography and basal friction in that region. Additionally, if lakes on the GrIS overflow, lakes in downstream catchments may receive extra water, and thus

surface catchment areas of lakes on the GrIS may enlarge through the melt season (Banwell and others, 2012a).

Conversely, undulations and depressions on ice shelves, which may fill to form lakes, are produced and influenced by an entirely different combination of processes. To date, only a few studies have focused on improving our understanding of lake formation processes on ice shelves. One such study is by LaBarbera and MacAyeal (2011), who suggest that supraglacial lakes on ice shelves form in the depressions of a viscous-buckling wave associated with compressive ice-shelf stresses. This idea is thought to be associated with a previously described ice-shelf phenomenon known as 'pressure rolls' (Hattersley-Smith, 1957; Collins and McCrae, 1985). As various studies have also concluded, when supraglacial lakes accumulate water, they begin to flex the ice shelf downward, causing further deepening and attraction of surrounding meltwater runoff patterns (Hattersley-Smith, 1957; MacAyeal and Sergienko, 2013). However, due to the minimal surface slope of ice shelves compared to the steep surface slope of the GrIS, only relatively small catchment areas are likely to develop on ice shelves.

Further to these ideas, we speculate that surface undulations on ice shelves may form as ice crosses the sudden break in slope at the grounding line, as here it is likely to experience some degree of flexure, buckling or fracturing. For example, ice-covered lakes and dolines were observed near the grounding line of the Lambert/Amery Ice Shelf by Hambrey and Dowdeswell (1994). It is also here (i.e. near the Antarctic Peninsula mountains) where surface melting is likely to be highest, owing to a föhn effect and/or runoff from darker, ice-free areas. As the ice subsequently converges away from the grounding line and out onto the ice shelf and towards the ice front, these undulations, which were probably parallel to the grounding line (if the ice-flow direction was perpendicular to the grounding line), may undergo strain and thus rotation in response to the convergence of ice flow and the resultant stress field. We suggest that it is the combination of these processes that assist in producing lakes on the LBIS which are relatively shallow and uniform in depth, and have an average orientation of 46° to the general ice-flow direction.

## 5. CONCLUSIONS

Compared to lakes at Paakitsoq, a land-terminating region of the GrIS, lakes on the floating LBIS show less variance in their mean depths and areas. It is therefore conceivable that the majority of lakes on the LBIS all reached a critical volume to drain by hydrofracture at a similar time, enabling the rapid break-up of the ice shelf in March 2002. Compared to lakes at Paakitsoq, lakes on the LBIS have a greater spatial density, and also cover a greater proportion of the total surface area of the ice on which the lakes are localized (~5.3% cf. ~1.0%). This greater density is probably due to the almost negligible large-scale elevation change across the surface of the ice shelf (~25 m) compared to a change of ~1100 m at Paakitsoq. As a consequence of the low variability of the surface elevation of the LBIS, it seems feasible that supraglacial lakes are hydrologically isolated (i.e. where water does not overflow from basins of different elevation) and simply grow in place by enhanced surface ablation associated with the reduced albedo of standing water.

Finally, if we consider the transferability of existing surface-routing and lake-filling models (e.g. Banwell and

others, 2012a; Leeson and others, 2012) to Antarctic ice shelves, we conclude that ice shelves are likely to be too flat to enable the widespread movement of meltwater across the surface and the filling of surface depressions to be coherently modelled. This is likely to mean that lakes on ice shelves can be modelled more simplistically, as features that derive their water from local drainage basins that are relatively static in size and shape. Additionally, existing surface-routing and lake-filling models assume static ice topography. Although this is a good assumption for the GrIS, where lake positions are relatively constant interannually, this is not a reasonable assumption for Antarctic ice shelves, where lakes move concurrently with ice flow and where lake water constitutes a surface load that introduces vertical flexure.

## ACKNOWLEDGEMENTS

We acknowledge the support of the US National Science Foundation under grant ANT-0944248. We also thank the scientific editor, Weili Wang, and two anonymous referees for careful reviews that helped to improve an earlier draft of the paper.

## REFERENCES

- Banwell AF, Arnold NS, Willis IC, Tedesco M and Ahlström AP (2012a) Modeling supraglacial water routing and lake filling on the Greenland Ice Sheet. *J. Geophys. Res.*, **117**(F4), F04012 (doi: 10.1029/2012JF002393)
- Banwell AF and 6 others (2012b) Calibration and evaluation of a high-resolution surface mass-balance model for Paakitsoq, West Greenland. *J. Glaciol.*, **58**(212), 1047–1062 (doi: 10.3189/2012JoG12J034)
- Banwell AF, Willis IC and Arnold NS (2013) Modeling subglacial water routing at Paakitsoq, W Greenland. *J. Geophys. Res.*, **118** (doi: 10.1002/jgrf.20093)
- Bartholomew ID and 6 others (2011) Seasonal variations in Greenland Ice Sheet motion: inland extent and behaviour at higher elevations. *Earth Planet. Sci. Lett.*, **307**(3–4), 271–278 (doi: 10.1016/j.epsl.2011.04.014)
- Box JE and Ski K (2007) Remote sounding of Greenland supraglacial melt lakes: implications for subglacial hydraulics. *J. Glaciol.*, **53**(181), 257–265 (doi: 10.3189/172756507782202883)
- Bromwich DH and 6 others (2013) Central West Antarctica among the most rapidly warming regions on Earth. *Nature Geosci.*, **6**(2), 139–145 (doi: 10.1038/ngeo1671)
- Chander G, Markham BL and Helder DL (2009) Summary of current radiometric calibration coefficients for Landsat MSS, TM, ETM+, and EO-1 ALI sensors. *Remote Sens. Environ.*, **113**(5), 893–903 (doi: 10.1016/j.rse.2009.01.007)
- Collins IF and McCrae IR (1985) Creep buckling of ice shelves and the formation of pressure rollers. *J. Glaciol.*, **31**(109), 242–252
- Darnell KN, Amundson JM, Cathles LM and MacAyeal DR (2013) The morphology of supraglacial lake ogives. *J. Glaciol.*, **59**(215), 533–544 (doi: 10.3189/2013JoG12J098)
- Das SB and 6 others (2008) Fracture propagation to the base of the Greenland Ice Sheet during supraglacial lake drainage. *Science*, **320**(5877), 778–781 (doi: 10.1126/science.1153360)
- Doyle SH and 9 others (2013) Ice tectonic deformation during the rapid in situ drainage of a supraglacial lake on the Greenland Ice Sheet. *Cryosphere*, **7**(1), 129–140 (doi: 10.5194/tc-7-129-2013)
- Echelmeyer K, Clarke TS and Harrison WD (1991) Surficial glaciology of Jakobshavn Isbræ, West Greenland: Part I. Surface morphology. *J. Glaciol.*, **37**(127), 368–382
- Fitzpatrick AAW and 9 others (2013) A decade of supraglacial lake volume estimates across a land-terminating margin of the Greenland Ice Sheet. *Cryos. Discuss.*, **7**(2), 1383–1414 (doi: 10.5194/tcd-7-1383-2013)

- Glasser NF and Gudmundsson GH (2012) Longitudinal surface structures (flowstripes) on Antarctic glaciers. *Cryosphere*, **6**(2), 383–391 (doi: 10.5194/tc-6-383-2012)
- Glasser NF and Scambos TA (2008) A structural glaciological analysis of the 2002 Larsen B ice-shelf collapse. *J. Glaciol.*, **54**(184), 3–16 (doi: 10.3189/002214308784409017)
- Glasser N and 7 others (2009) Surface structure and stability of the Larsen C ice shelf, Antarctic Peninsula. *J. Glaciol.*, **55**(191), 400–410 (doi: 10.3189/002214309788816597)
- Glasser NF, Scambos TA, Bohlander J, Truffer M, Pettit EC and Davies BJ (2011) From ice-shelf tributary to tidewater glacier: continued rapid recession, acceleration and thinning of Röhss Glacier following the 1995 collapse of the Prince Gustav Ice Shelf, Antarctic Peninsula. *J. Glaciol.*, **57**(203), 397–406 (doi: 10.3189/002214311796905578)
- Gudmundsson GH (2003) Transmission of basal variability to a glacier surface. *J. Geophys. Res.*, **108**(B5), 2253 (doi: 10.1029/2002JB0022107)
- Hambrey MJ and Dowdeswell JA (1994) Flow regime of the Lambert Glacier–Amery Ice Shelf system, Antarctica: structural evidence from Landsat imagery. *Ann. Glaciol.*, **20**, 401–406
- Hattersley-Smith G (1957) The rolls on the Ellesmere ice shelf. *Arctic*, **10**(1), 32–44
- Hoffman MJ, Catania GA, Neumann TA, Andrews LC and Rumrill JA (2011) Links between acceleration, melting, and supraglacial lake drainage of the western Greenland Ice Sheet. *J. Geophys. Res.*, **116**(F4), F04035 (doi: 10.1029/2010JF001934)
- Ingle JD and Crouch SR (1988) Spectrochemical measurements. In Ingle JD and Crouch SR eds. *Spectrochemical analysis*. Prentice Hall, Upper Saddle River, NJ
- Johansson AM, Jansson P and Brown IA (2013) Spatial and temporal variations in lakes on the Greenland Ice Sheet. *J. Hydrol.*, **476**, 314–320 (doi: 10.1016/j.jhydrol.2012.10.045)
- Joughin I and 9 others (2013) Influence of supraglacial lakes and ice-sheet geometry on seasonal ice-flow variability. *Cryos. Discuss.*, **7**(2), 1101–1118 (doi: 10.5194/tcd-7-1101-2013)
- LaBarbera CH and MacAyeal DR (2011) Traveling supraglacial lakes on George VI Ice Shelf, Antarctica. *Geophys. Res. Lett.*, **38**(24), L24501 (doi: 10.1029/2011GL049970)
- Lampkin DJ and Vanderberg J (2011) A preliminary investigation of the influence of basal and surface topography on supraglacial lake distribution near Jakobshavn Isbræ, western Greenland. *Hydrol. Process.*, **25**(21), 3347–3355 (doi: 10.1002/hyp.8170)
- Leeson AA, Shepherd A, Palmer S, Sundal A and Fettweis X (2012) Simulating the growth of supraglacial lakes at the western margin of the Greenland ice sheet. *Cryosphere*, **6**(5), 1077–1086 (doi: 10.5194/tc-6-1077-2012)
- Liang Y-L and 7 others (2012) A decadal investigation of supraglacial lakes in West Greenland using a fully automatic detection and tracking algorithm. *Remote Sens. Environ.*, **123**, 127–138 (doi: 10.1016/j.rse.2012.03.020)
- Lüthje M, Pedersen LT, Reeh N and Greuell W (2006) Modelling the evolution of supraglacial lakes on the West Greenland ice-sheet margin. *J. Glaciol.*, **52**(179), 608–618 (doi: 10.3189/172756506781828386)
- MacAyeal DR and Sergienko OV (2013) The flexural dynamics of melting ice shelves. *Ann. Glaciol.*, **54**(63 Pt 1), 1–10 (doi: 10.3189/2013AoG63A256)
- McGrath D, Steffen K, Rajaram H, Scambos T, Abdalati W and Rignot E (2012) Basal crevasses on the Larsen C Ice Shelf, Antarctica: implications for meltwater ponding and hydrofracture. *Geophys. Res. Lett.*, **39**(16), L16504 (doi: 10.1029/2012GL052413)
- Mobley CD (1994) *Light and water: radiative transfer in natural waters*. Academic Press, San Diego
- Phillips HA (1998) Surface meltstreams on the Amery Ice Shelf, East Antarctica. *Ann. Glaciol.*, **27**, 177–181
- Philpot WD (1989) Bathymetric mapping with passive multispectral imagery. *Appl. Opt.*, **28**(8), 1569–1578
- Rignot E and Thomas RH (2002) Mass balance of polar ice sheets. *Science*, **297**(5586), 1502–1506 (doi: 10.1126/science.1073888)
- Rott H, Müller F, Nagler T and Floricioiu D (2011) The imbalance of glaciers after disintegration of Larsen-B ice shelf, Antarctic Peninsula. *Cryosphere*, **5**(1), 125–134 (doi: 10.5194/tc-5-125-2011)
- Sandhäger H, Rack W and Jansen D (2005) Model investigations of Larsen B Ice Shelf dynamics prior to the breakup. *FRISP Rep.* 16, 5–12
- Scambos TA, Hulbe C, Fahnestock M and Bohlander J (2000) The link between climate warming and break-up of ice shelves in the Antarctic Peninsula. *J. Glaciol.*, **46**(154), 516–530 (doi: 10.3189/172756500781833043)
- Scambos T, Hulbe C and Fahnestock M (2003) Climate-induced ice shelf disintegration in the Antarctic Peninsula. In Domack EW, Burnett A, Leventer A, Conley P, Kirby M and Bindschadler R eds. *Antarctic Peninsula climate variability: a historical and paleoenvironmental perspective*. American Geophysical Union, Washington, DC, 79–92
- Scambos TA, Bohlander JA, Shuman CA and Skvarca P (2004) Glacier acceleration and thinning after ice shelf collapse in the Larsen B embayment, Antarctica. *Geophys. Res. Lett.*, **31**(18), L18402 (doi: 10.1029/2004GL020670)
- Scambos T and 7 others (2009) Ice shelf disintegration by plate bending and hydro-fracture: satellite observations and model results of the 2008 Wilkins ice shelf break-ups. *Earth Planet. Sci. Lett.*, **280**(1–4), 51–60 (doi: 10.1016/j.epsl.2008.12.027)
- Selmes N, Murray T and James TD (2011) Fast draining lakes on the Greenland Ice Sheet. *Geophys. Res. Lett.*, **38**(15), L15501 (doi: 10.1029/2011GL047872)
- Sergienko OV (2013) Glaciological twins: basally controlled subglacial and supraglacial lakes. *J. Glaciol.*, **59**(213), 3–8 (doi: 10.3189/2013JG12J040)
- Sergienko O and MacAyeal DR (2005) Surface melting on Larsen Ice Shelf, Antarctica. *Ann. Glaciol.*, **40**, 215–218 (doi: 10.3189/172756405781813474)
- Sneed WA and Hamilton GS (2007) Evolution of melt pond volume on the surface of the Greenland Ice Sheet. *Geophys. Res. Lett.*, **34**(3), L03501 (doi: 10.1029/2006GL028697)
- Sneed WA and Hamilton GS (2011) Validation of a method for determining the depth of glacial melt ponds using satellite imagery. *Ann. Glaciol.*, **52**(59), 15–20 (doi: 10.3189/172756411799096240)
- Tedesco M and 7 others (2012) Measurement and modeling of ablation of the bottom of supraglacial lakes in western Greenland. *Geophys. Res. Lett.*, **39**(2), L02502 (doi: 10.1029/2011GL049882)
- Tedesco M, Willis IC, Hoffman MJ, Banwell AF, Alexander P and Arnold NS (2013) Ice dynamic response to two modes of surface lake drainage on the Greenland ice sheet. *Environ. Res. Lett.*, **8**(3), 034007 (doi: 10.1088/1748-9326/8/3/034007)
- Thomsen HH, Thorning L and Braithwaite RJ (1988) Glacier-hydrological conditions on the Inland Ice north-east of Jakobshavn/Ilulissat, West Greenland. *Rapp. Grøn. Geol. Unders.* 138
- Van den Broeke M (2005) Strong surface melting preceded collapse of Antarctic Peninsula ice shelf. *Geophys. Res. Lett.*, **32**(12), L12815 (doi: 10.1029/2005GL023247)
- Van der Veen CJ (1998) Fracture mechanics approach to penetration of surface crevasses on glaciers. *Cold Reg. Sci. Technol.*, **27**(1), 31–47
- Van der Veen CJ (2007) Fracture propagation as means of rapidly transferring surface meltwater to the base of glaciers. *Geophys. Res. Lett.*, **34**(1), L01501 (doi: 10.1029/2006GL028385)
- Vaughan DG (2008) West Antarctic Ice Sheet collapse – the fall and rise of a paradigm. *Climatic Change*, **91**(1–2), 65–79 (doi: 10.1007/s10584-008-9448-3)
- Vieli A, Payne AJ, Du Z and Shepherd A (2006) Numerical modelling and data assimilation of the Larsen B ice shelf, Antarctic Peninsula. *Philos. Trans. R. Soc. London, Ser. A*, **364**(1844), 1815–1839 (doi: 10.1098/rsta.2006.1800)